PHYSICAL REVIEW B **92**, 140504(R) (2015)

# Probing superconductivity and pairing symmetry by coherent phonons in multiorbital superconductors

Chandan Setty,[1] Jimin Zhao,[2] and Jiangping Hu[1,2,3,*]

[1]*Department of Physics and Astronomy, Purdue University, West Lafayette, Indiana 47907, USA*

[2]*Beijing National Laboratory for Condensed Matter Physics, Institute of Physics, Chinese Academy of Sciences, Beijing 100090, China*

[3]*Collaborative Innovation Center of Quantum Matter, Beijing 100871, China*

(Received 16 March 2015; revised manuscript received 20 June 2015; published 21 October 2015)

We show that the phase information contained in coherent phonon oscillations generated by a laser pulse in a multiorbital superconductor can be used as an experimental tool to probe superconductivity and pairing symmetries. The phase difference between the normal and superconducting states is proportional to the superconducting order parameter just below the superconducting transition temperature $T_c$. It also exhibits different behaviors for superconducting states with different pairing symmetries. In particular, if there is an orbital-dependent internal sign change state, the phase difference can have a discontinuous jump below $T_c$.

DOI: 10.1103/PhysRevB.92.140504 PACS number(s): 74.20.Rp, 74.25.Kc, 74.25.nd, 74.70.Xa

## I. INTRODUCTION

The superconductivity in a multiband electronic system can be extremely rich and complex. Many recently discovered correlated electron systems belong to this category of multiband superconductors. For example, iron-based superconductors discovered six years ago [1] have multiple Fermi surfaces and their bands near the Fermi level are attributed to all five $d$ orbitals. These materials exhibit a variety of intriguing properties associated with all of the degrees of freedom including charge, orbital, spin, and lattice [2], which can, in principle, lead to many possible novel superconducting states [3].

While theoretically, a multiband structure is a fertile ground for new physics, in experiments it is still very difficult to detect them and determine their mechanisms because of the involvement of the multiple degrees of freedom. In such multiorbital superconductors (see, e.g., Ref. [4]), experimental observations can be subject to multiple interpretations, and the intricate interplay among electronic states such as nematicity, magnetism, and orbital ordering is a subject of active research [5,6]. The pairing symmetry in multiorbital superconducting states, arguably the most important property, is still controversial and highly debated [3]. While the magnitude of the superconducting order parameter can be directly probed by many experimental techniques, such as angle-resolved photoemission spectra (ARPES) and scanning tunneling microscopy (STM), there are few good direct probes of the phase distribution of the superconducting order parameter across their multiorbital Fermi surface. In particular, when the phase distribution is not enforced by the symmetry of the superconducting state, as the case stands in many theoretically proposed states in multiorbital superconductors, the phase sensitive junction techniques [7] that determined the $d$-wave pairing symmetry in cuprates are also not applicable.

For the last couple of decades, ultrafast pump-probe spectroscopy has played an increasing role in probing the superconducting ground state, with the high $T_c$ cuprates having grabbed much of the attention [8–27], along with a few experiments performed on multiorbital iron superconductors [28–38] as well. The primary focus of most of these experiments has been the measurement of relaxation times that can be extracted from the behavior of the change in reflectivity $\frac{\Delta R}{R}$ of the probe pulse as a function of the delay time $\delta$ between the pump and the probe. From this, one can indirectly obtain information about the strength of the electron-phonon couplings and their anisotropies [11,12], the density of photoexcited quasiparticles [19,25], pseudo- and superconducting gaps [25], and signatures of the origin of the superconducting interaction [15]. However, even though coherent phonon oscillations in ultrafast experiments have been generated [14,36] and studied [32,34] for a while now, only a few experimental works have addressed the role of the superconducting phase on these oscillations and no theoretical background has been laid.

In this Rapid Communication, we show that the phase of these coherent phonon oscillations contains useful information about the superconducting phase and its pairing symmetry; in particular, we show that the difference in the phase of the oscillations between the normal and superconducting state is proportional to the superconducting gap, and, in certain scenarios, can help distinguish the sign change of superconducting orders on different bands. Thus, the coherent phonons can act as an experimental probe of superconducting symmetries.

## II. THEORY

The coherent phonon amplitude mode with wave vector $q$ is described by the driven harmonic oscillator [39,40]

$$\frac{d^2Q_q}{dt^2} + 2\beta\frac{dQ_q}{dt} + \Omega^2 Q_q = F(t), \tag{1}$$

where $Q_q$ is the amplitude of the phonon mode, $\Omega$ is the frequency of the oscillator, $\beta$ is the damping parameter, and $F(t)$ is the driving force. The solution to the above equation is given by

$$Q_q(t) = \mathcal{A}e^{-\beta t}\cos(\tilde{\Omega}t + \Gamma_{\rm ph}), \tag{2}$$

*jphu@iphy.ac.cn

 

where $\tilde{\Omega} = \sqrt{\Omega^2 - \beta^2}$ and $\mathcal{A}$ is the amplitude of the oscillation which is proportional to the magnitude of the driving force $F$. For simplicity, we will ignore any effect of damping. In such a case, the phase of the phonon oscillation $\Gamma_{\rm ph}$ is given by [40]

$$\tan(\Gamma_{\rm ph}) = \frac{\mathrm{Im}[iF(-\Omega)]}{\mathrm{Re}[iF(-\Omega)]}. \tag{3}$$

The driving force $F(t)$ can be derived microscopically under reasonable approximations. Consider a general Hamiltonian that describes the physical processes in an ultrafast pump-probe experiment given by

$$H = H_e + H_p + H_{ep} + H_{el}(t), \tag{4}$$

where $H_e$, $H_p$, $H_{ep}$, and $H_{el}(t)$ are electronic, phononic, electron-phonon coupling, and electron-pulse interaction parts, respectively [39]. In a superconducting state, the electronic part $H_e$ is given by the general BCS form

$$H_e = \sum_{k\sigma\alpha\beta} \epsilon_{k\sigma\alpha\beta} c^\dagger_{k\sigma\alpha} c_{k\sigma\beta} + \sum_{k\alpha} \Delta_{k\alpha} c^\dagger_{k\alpha\uparrow} c^\dagger_{-k\alpha\downarrow}, \tag{5}$$

where $\alpha$ and $\sigma$ are the orbital and spin indices. We take the standard form for $H_p = \frac{1}{2}\sum_q (P_q^2 + \Omega_q^2 Q_q^2)$ and $H_{ep} = \sum_{kq\alpha\alpha'} \xi_{\alpha\alpha'} Q_q c^\dagger_{k\alpha} c_{k+q\alpha'} + \text{H.c.}$, where $Q_q$ and $P_q$ are the canonical coordinates and momenta. The time-dependent electron-laser pulse interaction is given by $H_{el}(t) = \sum_{kq\alpha\alpha'} V_{\alpha\alpha'}(t) c^\dagger_{k\alpha} c_{k+q\alpha'} + \text{H.c.}$, with $V_{\alpha\alpha'}(t) = \frac{e}{m}\int dr_i \phi_\alpha(r_i)^* [\vec{A}(t)\cdot\vec{p}_i]\phi_{\alpha'}(r_i)$. As the coherent phonons are generated at $q = 0$ and the momentum of the light is much smaller than the electron momentum, we can set $q = 0$ in all of the above Hamiltonians.

We consider parameters in a typical femtosecond pump-probe experiment. The pump pulse (central frequency $\omega_o \sim$ 375 THz) has a width of $\tau \sim 80$ fs and a relatively broad spectral width of the order of $\Delta\nu \sim$ 5–10 THz. Such a spectral width is just enough to excite the lowest energy optical phonon mode whose energy is around $\Omega \sim 5$ THz. To ensure that the phonon oscillations are properly resolved in time, the width of the pump laser pulse satisfies the condition $\tau \ll \Omega^{-1}$.

The average force driving the coherent phonon oscillations is given by $F(t) = -\partial\langle H_{e-p}\rangle(t)/\partial Q_{\vec{q}}$. Here, $\langle\cdots\rangle$ denotes an ensemble average over eigenstates of $H - H_{el}(t)$ time evolving in $H_{el}(t)$ perturbatively. In line with Ref. [40], we assume that the electric field is spatially homogeneous and Gaussian centered around $\omega_o$. Thus the electric field product $E(\omega)E(\omega+\Omega)$ is strongly peaked at $\omega_o - \Omega/2$. This leads to an expression for the driving force [39,40],

$$F(\Omega) = \frac{-C}{\left(\omega_o^2 - \frac{\Omega^2}{4}\right)} \sum_{\vec{k}mn} \left( \frac{\tilde{\xi}_{In}\tilde{V}_{nm}(\vec{k})\tilde{V}_{mI}(\vec{k})}{(\omega_{nI} - \Omega - ig)(\omega_{mI} - \omega_o - ig)} + \frac{\tilde{\xi}_{nI}\tilde{V}_{mn}(\vec{k})\tilde{V}_{Im}(\vec{k})}{(\omega_{nI} + \Omega + ig)(\omega_{mI} - \omega_o + ig)} \right). \tag{6}$$

Here, $n,m,I$ are band states, $C$ is an unimportant constant, $g$ contributes to the optical absorption, and $\vec{k}$ is the crystal momentum. We have defined $\omega_{nI} \equiv \omega_{nI}(\vec{k}) = \omega_n - \omega_I$, where $\omega_n$ is the energy of band $n$ with momentum $\vec{k}$. The tilde sign above the matrix elements denotes the respective quantities written in the band basis. In the expression for $F(\Omega)$, we have assumed that the laser frequency is the largest energy scale in the problem. Therefore, we have chosen to keep the most resonant terms by ignoring a third term which has a denominator proportional to $\omega_o^2$.

## III. TWO BAND MODEL

Our goal in this section is to study the phase of the coherent phonon oscillations ($\Gamma_{\rm ph}$) across $T_c$ for a generic two orbital model. Our model comprises intraorbital hoppings $\epsilon_1(\vec{k})$,$\epsilon_2(\vec{k})$, and the interorbital hopping $\epsilon_{12}(\vec{k}) \equiv m_k$. For analytic simplicity, we choose the two orbitals to have the same complex gap order parameter $|\Delta|e^{i\phi}$. This condition will be relaxed in the next section where we apply numerics. For the electron-phonon couplings, we only keep nonzero matrix elements for the coupling between the two different orbitals ($\xi'$) and coupling between superconducting particle-hole bands ($\xi e^{i\phi}$). We can write out these operators in the matrix form with the electronic part of the Hamiltonian in the superconducting state described by [in the basis $\hat{\mathcal{C}}_k = (c_{k1\uparrow}, c_{k2\uparrow}, c^\dagger_{-k1\downarrow}, c^\dagger_{-k2\downarrow})$]

$$\hat{\mathcal{H}}_e = \sum_k \hat{\mathcal{C}}_k^\dagger \begin{pmatrix} \epsilon_{1k} & m_k & \Delta e^{i\phi} & 0 \\ m_k & \epsilon_{2k} & 0 & \Delta e^{i\phi} \\ \Delta e^{-i\phi} & 0 & -\epsilon_{1k} & -m_k \\ 0 & \Delta e^{-i\phi} & -m_k & -\epsilon_{2k} \end{pmatrix} \hat{\mathcal{C}}_k, \tag{7}$$

where $\epsilon_1(\vec{k})$, $\epsilon_2(\vec{k})$, and $m_k$ are the orbital matrix elements described previously. We choose a symmetric gap on the two orbitals given by $\Delta_1 = \Delta_2 = \Delta e^{i\phi}$, where $\phi$ is the phase of the superconducting condensate and $\Delta$ is positive. The transformation matrix which diagonalizes such a Hamiltonian is given by

$$U = \begin{pmatrix} -c_\theta s_{\beta-} e^{i\phi} & -s_\theta s_{\beta+} e^{i\phi} & s_\theta c_{\beta+} e^{i\phi} & c_\theta c_{\beta-} e^{i\phi} \\ s_\theta s_{\beta-} e^{i\phi} & -c_\theta s_{\beta+} e^{i\phi} & c_\theta c_{\beta+} e^{i\phi} & -s_\theta c_{\beta-} e^{i\phi} \\ c_\theta c_{\beta-} & s_\theta c_{\beta+} & s_\theta s_{\beta+} & c_\theta s_{\beta-} \\ -s_\theta c_{\beta-} & c_\theta c_{\beta+} & c_\theta s_{\beta+} & -s_\theta s_{\beta-} \end{pmatrix}, \tag{8}$$

where $c$ and $s$ stand for sine and cosine and all the phases being momentum dependent along with the following definitions:

$$\tan 2\theta(\vec{k}) = \frac{2m_k}{\epsilon_{2k} - \epsilon_{1k}},$$

$$\sin\beta_\pm(\vec{k}) = \sqrt{\frac{1}{2}\left(1 - \frac{\epsilon_\pm(\vec{k})}{E_\pm(\vec{k})}\right)} = \frac{\Delta}{\sqrt{\Delta^2 + \mathscr{E}_\pm^2}},$$

$$\epsilon_\pm(\vec{k}) = \frac{1}{2}\left[\epsilon_{1k} + \epsilon_{2k} \pm \sqrt{(\epsilon_{1k} - \epsilon_{2k})^2 + 4m_k^2}\right],$$

$$E_\pm(\vec{k}) = \sqrt{\Delta^2 + \epsilon_\pm(\vec{k})^2},$$

$$\mathscr{E}_\pm = \epsilon_\pm(\vec{k}) + E_\pm(\vec{k}).$$

The eigenvalues appearing after the diagonalization are given by $\pm E_\pm(\vec{k})$. The matrix for the electron-phonon coupling is

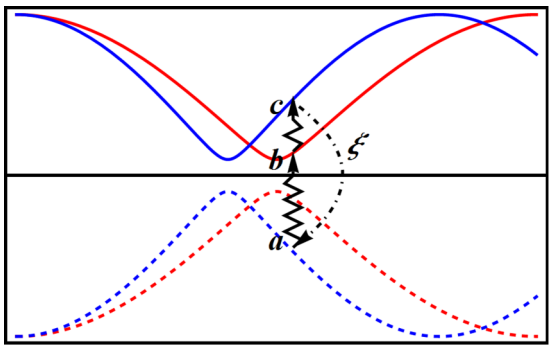


FIG. 1. (Color online) A cartoon plot showing the toy band structure used to illustrate the scattering between superconducting bands close to the Fermi level. A quasiparticle is light scattered (solid wavy line) from an occupied band state $a$ to an empty state in band state $b$ and light scattered again from band state $b$ to another band state $c$. Finally, the quasiparticle makes a transition back to the band state $a$ by scattering with a phonon (dashed-dotted line). The energy scale on the vertical axis is of the order of the superconducting gap.

chosen as (in the same orbital basis as above)

$$\hat{\xi} = \begin{pmatrix} 0 & \xi' & \xi e^{i\phi} & 0 \\ \xi' & 0 & 0 & \xi e^{i\phi} \\ \xi e^{-i\phi} & 0 & 0 & -\xi' \\ 0 & \xi e^{-i\phi} & -\xi' & 0 \end{pmatrix}. \tag{9}$$

Here, $\xi$ and $\xi'$ are constants so that the phonon matrix elements in the superconducting band basis can be evaluated easily. As the electronic response to the laser pulse is a very fast process, we can assume that the phonon is not activated during the laser pulse excitation. Such an approximation is easy to justify considering that the fast moving electrons have a larger effect on the slow moving nuclei than the other way around—an analog of the Born-Oppenheimer approximation in atomic physics. In this case, the lowest order effect of the electron-phonon coupling is in the form of the driving force, $F(t) = -\partial\langle H_{ep}\rangle(t)/\partial Q_{\vec{q}}$.

We now proceed with our calculation of the average driving force $F(t)$. To bring out the physics essential for our discussion, we consider a scattering process illustrated in the cartoon in Fig. 1. A quasiparticle in the state $a$ is scattered by a photon to the empty state $b$ above the Fermi level, and then scattered again into another empty state $c$ by a second photon. Finally, the quasiparticle is scattered back to its original state $a$ through a phonon or a series of phonons. We explicitly evaluate the matrix element product $\tilde{\xi}_{ac}\tilde{V}_{cb}(\vec{k})\tilde{V}_{ba}(\vec{k})$ for such a process so that other similar scattering processes can be determined analogously. The tilde sign appearing on the top denotes that the matrix elements are written in the superconducting band basis and need to be converted into the orbital basis. To do this, we first have to perform an unitary transform into the orbital basis and then use the formulas described in Ref. [41] for tight binding matrix elements. In the process of this conversion, the matrix elements pick up coherence factors which depend on the superconducting order parameter $\Delta$. This dependence of the matrix elements on the order parameter is analogous to calculations done for experiments such as NMR, ultrasound, and neutron scattering. We can now proceed to evaluate the momentum matrix elements appearing in $\tilde{\xi}_{ac}\tilde{V}_{cb}\tilde{V}_{ba}$ using the general formulas [41]

$$\begin{aligned}\langle n,k|\vec{p}|m,k\rangle = &\sum_{\alpha,\beta} u_{n\beta}(\vec{k})^* u_{m\alpha}(\vec{k})\nabla_{\vec{k}}\langle\beta,k|H|\alpha,k\rangle \\ &+ i(E_{nk} - E_{mk})\sum_{\alpha\beta} u_{n\beta}(\vec{k})^* \\ &\times u_{m\alpha}(\vec{k})\langle\beta,0|\vec{r}|\alpha,0\rangle,\end{aligned}$$

where $\alpha,\beta$ run over orbitals and $n,m$ denoted the band index. $u_{m\alpha}$ are the matrix elements of the transformation matrix $U$ and $\langle\beta,0|\vec{r}|\alpha,0\rangle$ are the intraunit cell matrix elements of the position operator. We consider a single Fe unit cell and all the position matrix elements between $d$ orbitals go to zero. To maintain analytical tractability in the analysis to follow, we only keep derivatives of $m_k$ in the momentum matrix elements; inclusion of the other terms does not change the conclusions of our results but only yields bulky expressions that do not add any new physics. With these assumptions, we can evaluate the matrix element product as

$$\begin{aligned}\tilde{\xi}_{ac}\tilde{V}_{cb}\tilde{V}_{ba} &= f(\theta_k)\sin(\beta_+ + \beta_-)\cos(\beta_+ + \beta_-)(\xi\cos(2\beta_-) + \xi'\sin 2\theta_k \sin 2\beta_-) \\ &= f(\theta_k)\left(\frac{\mathscr{E}_-\Delta + \mathscr{E}_+\Delta}{\sqrt{\Delta^2+\mathscr{E}_+^2}\sqrt{\Delta^2+\mathscr{E}_-^2}}\right)\left(\frac{\mathscr{E}_+\mathscr{E}_- - \Delta^2}{\sqrt{\Delta^2+\mathscr{E}_+^2}\sqrt{\Delta^2+\mathscr{E}_-^2}}\right)\left(\xi\left[\frac{\mathscr{E}_-^2-\Delta^2}{\mathscr{E}_-^2+\Delta^2}\right] + \xi'\sin 2\theta_k\left[\frac{2\Delta\mathscr{E}_-}{\mathscr{E}_-^2-\Delta^2}\right]\right),\end{aligned}$$

where $f(\theta_k)$ are band-structure-dependent functions and $\Delta$ is positive. Defining $x_\pm = \sqrt{\Delta^2+\mathscr{E}_\pm^2}$, we can write the above matrix element product as

$$\tilde{\xi}_{ac}\tilde{V}_{cb}(\vec{k})\tilde{V}_{ba}(\vec{k}) = \Delta\frac{f(\theta_k)}{x_+^2x_-^4}(\mathscr{E}_+ + \mathscr{E}_-)(\mathscr{E}_+\mathscr{E}_- - \Delta^2)[\xi(\mathscr{E}_-^2 - \Delta^2) + \xi'\sin 2\theta_k(2\Delta\mathscr{E}_-)], \tag{10}$$

where $f(\theta_k) = -(\partial m_k)^2\cos^2 2\theta_k$, $\mathscr{E}_\pm$, $E_\pm(\vec{k})$, the tangent of the band angle ($\tan 2\theta_k$), and $\epsilon_\pm(\vec{k})$ have all been defined previously. All the other matrix elements can be obtained in a similar fashion. From the above expression for the matrix element product, we can separate the most dominant contributions from different regions of the Brillouin zone. We consider three different cases: (1) contributions from momentum space points far away from the Fermi surface where $\epsilon_\pm(\vec{k}) \gg |\Delta| > 0$, (2) on the Fermi surface $\epsilon_+(\vec{k}) = 0 < |\Delta| \ll \epsilon_-(k)$, and finally (3) on the Fermi surface $\epsilon_-(\vec{k}) = 0 < |\Delta| \ll \epsilon_+(k)$. In these limits we can make the following approximate substitutions: (1) $x_\pm \sim \mathscr{E}_\pm$ for $\epsilon_\pm \gg \Delta > 0$, (2) $\mathscr{E}_+ \sim \Delta$, $x_- \sim \mathscr{E}_-$, $x_+ \sim \sqrt{2}\Delta$ for $\epsilon_- \gg \Delta > 0 = \epsilon_+$,

and finally (3) $\mathscr{E}_- \sim \Delta$, $x_+ \sim \mathscr{E}_+$, $x_- \sim \sqrt{2}\Delta$ for $\epsilon_+ \gg \Delta > 0 = \epsilon_-$. We find that

$$\tilde{\xi}_{ac}\tilde{V}_{cb}(\vec{k})\tilde{V}_{ba}(\vec{k}) = f(\theta_k) \times \begin{cases} \xi\frac{|\Delta|}{\tilde{\epsilon}}\left(1+\frac{2|\Delta|}{\mathscr{E}_-}\frac{\xi'}{\xi}s_{2\theta}\right), & \epsilon_\pm \gg |\Delta| > 0, \\ \frac{\xi}{2}\left(1+\frac{2|\Delta|}{\mathscr{E}_-}\frac{\xi'}{\xi}s_{2\theta}\right), & \epsilon_- \gg |\Delta| > 0 = \epsilon_+, \\ \frac{\xi'}{2}s_{2\theta}, & \epsilon_+ \gg |\Delta| > 0 = \epsilon_-, \end{cases} \tag{11}$$

where we have defined the effective band energy $\tilde{\epsilon} = \frac{\mathscr{E}_+\mathscr{E}_-}{\mathscr{E}_+ + \mathscr{E}_-}$ and $s_{2\theta} \equiv \sin 2\theta_k$. Similar expressions can be obtained for the other scattering processes. The energy denominators appearing in the expression for the driving force in Eq. (6) depend quadratically on the energy gap. From this, along with the expression for the matrix element product [written in Eq. (11)], we arrive at the central result of this section—*the coherent phonon phase encodes the behavior of the superconducting order parameter.* For small $\Delta$, the phase can be written very generally as $\Gamma_{\rm ph} = \alpha_1 + \alpha_2\Delta(T)$, where $\alpha_1$ and $\alpha_2$ are constants independent of temperature. As a result, the phase difference between the superconducting and normal state is proportional to the pairing gap. We also additionally conclude that the contribution to the average driving force from the momentum points far away from the Fermi surface is of $O(\Delta/\tilde{\epsilon})$ smaller than the contribution from those close to the Fermi surfaces. However, all the regions in the Brillouin zone contribute to the phase of the oscillation to the same order. This naturally implies that for a significant driving force to be generated, we would require the frequency of the phonon mode excited (∼5–10 THz) to be of the order of the superconducting gap. This is a condition that is hard to attain in classic BCS superconductors, but is comfortably satisfied by high temperature multiorbital superconductors.

## IV. THREE BAND MODEL: NUMERICS

To further test the above results, we consider a more realistic band model that describes multiorbital superconductors and study the pairing symmetry dependence. We also examine any signatures that can capture the interorbital sign change contained in the phase of coherent phonon oscillation. To illustrate our numerical results and maintain analytical tractability, we choose the three band model proposed by Daghofer *et al.* [42]. Figure 2 shows our result for the temperature dependence plot of the phase difference $\Gamma_S - \Gamma_N$ between the superconducting and normal states across $T_c$. The phase is a constant above $T_c$ and varies below it due to the development of a superconducting gap on the Fermi surfaces.

For a simple constant $s$-wave pairing (Fig. 2, left), the variation of the phase in the superconducting (SC) state is maximum at $T = 0$ (for small values of the gap) and follows a *linear* dependence on $\Delta$, as was analytically derived in the previous section. However, on increasing the magnitude of $\Delta$, the change in phase develops a maximum at a temperature $0 < T < T_c$ and then falls off at $T = 0$ due to higher order contributions of $\Delta$. Figure 2 (right) shows the plot of the phase of the oscillation as a function of temperature for different pairing symmetries. For the $s$-wave cases, there is a substantial change in the phase between $T = 0$ and $T = T_c$, whereas for the $d$-wave cases there is little phase change between $T = 0$ and $T = T_c$. In the $d$-wave scenario, the phase sharply plunges on entering into the superconducting state.

Figure 3 (top row) shows a color plot of the real part of $iF$ as a function of temperature and the absorption coefficient $g$. The left column corresponds to the case where the sign of the gap on all the three orbitals is the same $(+++$ case), while that on the right has a gap on the $xy$ orbital opposite in sign to that of the $xz$ and $yz$ orbitals $(++-$ case). Figure 3 (center row) shows cuts corresponding to different values of $g$ for both these cases. Clearly, below $T_c$, the slope of the real part of $iF$ has an opposite sign for the $(+++)$ and $(++-)$ cases. More specific to the three orbital model, the real part of $iF$ goes through a zero for the $(++-)$ case and therefore has a $\pi$ discontinuity in the phase. On the other hand, in the $(+++)$ scenario, the real part of $iF$ does not change sign and results in a smooth variation of phase with temperature (see Fig. 3, bottom row).

To get the physics governing the numerics above, we consider the three band model with a definite sign of the gap on the $xz$ and $yz$ orbitals (denoted by $\Delta_1 = \Delta$ and $\Delta_2 = \Delta$) and an arbitrary gap $\Delta_3$ on the $xy$ orbital. We find that for small values of $\Delta_3$, the driving force on the phonons can be written as $F(T) = \sum_{\vec{k}}[\tilde{\alpha}_1(k) + \mathrm{sgn}(\Delta\Delta_3)\tilde{\beta}_1(k)|\Delta_3(T)|] + i(\tilde{\alpha}_2(k) + \mathrm{sgn}(\Delta\Delta_3)\tilde{\beta}_2(k)|\Delta_3(T)|)$. Here, $\tilde{\alpha}_i$ and $\tilde{\beta}_i$ are band-structure-dependent functions which can be determined for a given model. For the above model, we find that $\sum_{\vec{k}}\tilde{\alpha}_2(\vec{k})$ and $\sum_{\vec{k}}\tilde{\beta}_2(\vec{k})$ are both negative. This implies that when all the three orbitals have the same sign of the gap, the real part of $iF(T)$ is negative. On the other hand, if the sign change exists

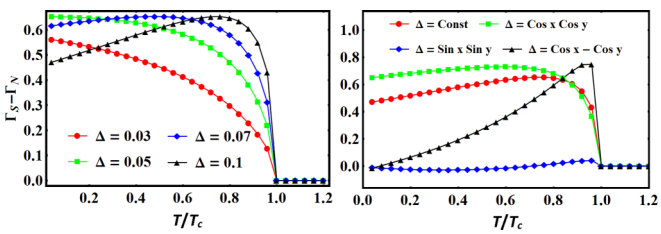


FIG. 2. (Color online) Plot showing the variation of the phase ($\Gamma_{\rm ph}$) difference between the superconducting (S) and normal (N) state as a function of temperature across $T_c$. Left: Phase as a function of magnitude of a constant $s$-wave gap on all the three bands. Right: Phase for different pairing forms of the gap, all the same on the three bands. The values of the electron-phonon coupling are chosen as $\xi' = 0.4$ eV for interorbital, $\xi'/4$ for $xz/yz$, and $\xi'/2$ for $xy$ intraorbital coupling, and the damping coefficient is chosen as $g = 0.3$ eV. The laser and phonon frequencies are fixed at 2 and 0.2 eV, respectively.

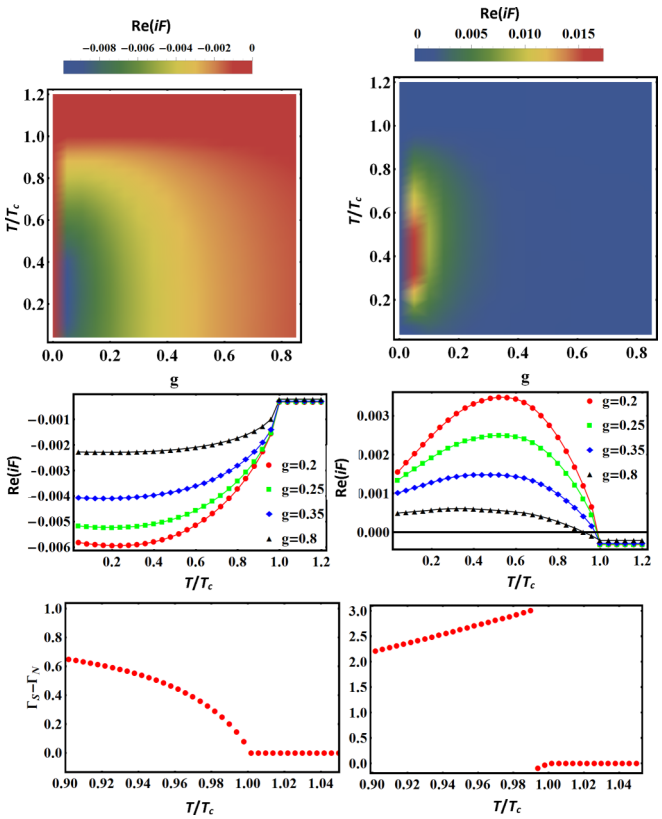


FIG. 3. (Color online) Plot showing the variation of the real part of the driving force $iF$ as a function of temperature (vertical axis) and the damping constant $g$ (horizontal axis) in the three orbital model of Ref. [42]. Top row left (right): Case where the signs of the gap on the $xz, yz$ orbitals are the same (opposite) as those on the $xy$ orbital. The color scale represents the real part of the driving force $iF$. Center row (left and right): Cuts along different chosen values of $g$ for the corresponding color plots above them. Bottom row: The corresponding phases as a function of temperature for the $g = 0.2$ case. The values of the electron-phonon couplings, and laser and phonon frequencies are chosen to be the same as in Fig. 2.

among the third orbitals, the denominator becomes zero for a critical temperature and results in an observable $\pi$ phase jump.

The above results can be applied to investigate the pairing symmetries in multiorbital superconductors. Here, we specifically discuss its applications to iron-based superconductors. Different pairing symmetries, including $s$-wave [43–48] and $d$-wave pairing symmetries [49,50], were proposed for different families of these multiorbital superconductors. Even within the $s$-wave pairing symmetry, there are a variety of possibilities on the internal sign changes, including the sign changes between different pockets (so called $s^{\pm}$ [43–46]) and between bands featured by different orbitals (so called orbital-dependent $S^{\pm}$ or antiphase $s^{\pm}$ [51–54]). Our results suggest that the phase of coherent phonons should have distinct behaviors with respect to the $s\pm$, antiphase-$s^{\pm}$, and $d$-wave states. In particular, as shown in Fig. 3, if a phase jump can be observed below $T_c$, it should be a smoking-gun signature for the antiphase-$s^{\pm}$ state.

Although our work focuses on superconducting states in multiorbital superconductors, it is important to note that it can be easily extended to study possible signatures of other types of order parameters, such as spin-density wave or charge-density wave, in many multiorbital systems.

## V. CONCLUSIONS

We have shown that coherent phonon oscillations can be an experimental probe of the superconducting state and its pairing symmetry. The phase of the coherent phonon carries intrinsic information of superconducting order parameters and can be applied to determine the pairing symmetries in complex multiorbital superconductors.

## ACKNOWLEDGMENTS

J.P.H. acknowledges support from the following grants: MOST of China (2012CB821400, 2015CB921300), NSFC (11190020, 91221303, 11334012), and Strategic Priority Research Program (B) of the Chinese Academy of Sciences (XDB07020200). J.M.Z. is supported by NSFC (11274372) and MOST of China (2012CB821402).

[1] Y. Kamihara, T. Watanabe, M. Hirano, and H. Hosono, J. Am. Chem. Soc. **130**, 3296 (2008).
[2] D. C. Johnston, Adv. Phys. **59**, 803 (2010).
[3] P. Hirschfeld, M. Korshunov, and I. Mazin, Rep. Prog. Phys. **74**, 124508 (2011).
[4] G. Stewart, Rev. Mod. Phys. **83**, 1589 (2011).
[5] R. Fernandes, A. Chubukov, and J. Schmalian, Nat. Phys. **10**, 97 (2014).
[6] P. Dai, J. Hu, and E. Dagotto, Nat. Phys. **8**, 709 (2012).
[7] D. Van Harlingen, Rev. Mod. Phys. **67**, 515 (1995).
[8] R. A. Kaindl, M. A. Carnahan, D. S. Chemla, S. Oh, and J. N. Eckstein, Phys. Rev. B **72**, 060510 (2005).
[9] C. Giannetti, G. Coslovich, F. Cilento, G. Ferrini, H. Eisaki, N. Kaneko, M. Greven, and F. Parmigiani, Phys. Rev. B **79**, 224502 (2009).
[10] R. Saichu, I. Mahns, A. Goos, S. Binder, P. May, S. Singer, B. Schulz, A. Rusydi, J. Unterhinninghofen, and D. Manske, Phys. Rev. Lett. **102**, 177004 (2009).
[11] L. Perfetti, P. A. Loukakos, M. Lisowski, U. Bovensiepen, H. Eisaki, and M. Wolf, Phys. Rev. Lett. **99**, 197001 (2007).
[12] F. Carbone, D.-S. Yang, E. Giannini, and A. H. Zewail, Proc. Natl. Acad. Sci. U.S.A. **105**, 20161 (2008).
[13] M. Schneider, J. Demsar, Y. Glinka, A. Klimov, A. Krapf, S. Rast, Y. Ren, W. Si, Y. Xu, and X. Zeng, Europhys. Lett. **60**, 460 (2002).
[14] W. Albrecht, T. Kruse, and H. Kurz, Phys. Rev. Lett. **69**, 1451 (1992).
[15] P. Kusar, V. V. Kabanov, J. Demsar, T. Mertelj, S. Sugai, and D. Mihailovic, Phys. Rev. Lett. **101**, 227001 (2008).

[16] G. Bianchi, C. Chen, M. Nohara, H. Takagi, and J. F. Ryan, Phys. Rev. B **72**, 094516 (2005).
[17] P. Kusar, J. Demsar, D. Mihailovic, and S. Sugai, Phys. Rev. B **72**, 014544 (2005).
[18] E. E. M. Chia, J.-X. Zhu, D. Talbayev, R. D. Averitt, A. J. Taylor, K.-H. Oh, I.-S. Jo, and S.-I. Lee, Phys. Rev. Lett. **99**, 147008 (2007).
[19] V. V. Kabanov, J. Demsar, and D. Mihailovic, Phys. Rev. Lett. **95**, 147002 (2005).
[20] J. P. Hinton, J. D. Koralek, Y. M. Lu, A. Vishwanath, J. Orenstein, D. A. Bonn, W. N. Hardy, and R. Liang, Phys. Rev. B **88**, 060508(R) (2013).
[21] C. J. Stevens, D. Smith, C. Chen, J. F. Ryan, B. Podobnik, D. Mihailovic, G. A. Wagner, and J. E. Evetts, Phys. Rev. Lett. **78**, 2212 (1997).
[22] N. Gedik, P. Blake, R. C. Spitzer, J. Orenstein, R. Liang, D. A. Bonn, and W. N. Hardy, Phys. Rev. B **70**, 014504 (2004).
[23] G. P. Segre, N. Gedik, J. Orenstein, D. A. Bonn, R. Liang, and W. N. Hardy, Phys. Rev. Lett. **88**, 137001 (2002).
[24] N. Gedik, J. Orenstein, R. Liang, D. A. Bonn, and W. N. Hardy, Science **300**, 1410 (2003).
[25] V. V. Kabanov, J. Demsar, B. Podobnik, and D. Mihailovic, Phys. Rev. B **59**, 1497 (1999).
[26] D. Dvorsek, V. V. Kabanov, J. Demsar, S. M. Kazakov, J. Karpinski, and D. Mihailovic, Phys. Rev. B **66**, 020510(R) (2002).
[27] J. Demsar, B. Podobnik, V. V. Kabanov, T. Wolf, and D. Mihailovic, Phys. Rev. Lett. **82**, 4918 (1999).
[28] C. Bonavolontà, L. Parlato, G. Pepe, C. De Lisio, M. Valentino, E. Bellingeri, I. Pallecchi, M. Putti, and C. Ferdeghini, Supercond. Sci. Technol. **26**, 075018 (2013).
[29] C. Luo, I. Wu, P. Cheng, J. Lin, K. Wu, T. Uen, J. Juang, T. Kobayashi, Y. Wen, and T. Huang, New J. Phys. **14**, 103053 (2012).
[30] C. W. Luo, I. H. Wu, P. C. Cheng, J.-Y. Lin, K. H. Wu, T. M. Uen, J. Y. Juang, T. Kobayashi, D. A. Chareev, O. S. Volkova, and A. N. Vasiliev, Phys. Rev. Lett. **108**, 257006 (2012).
[31] Elbert E. M. Chia, D. Talbayev, Jian-Xin Zhu, H. Q. Yuan, T. Park, J. D. Thompson, C. Panagopoulos, G. F. Chen, J. L. Luo, N. L. Wang, and A. J. Taylor, Phys. Rev. Lett. **104**, 027003 (2010).
[32] S. Kumar, L. Harnagea, S. Wurmehl, B. Buchner, and A. Sood, Europhys. Lett. **100**, 57007 (2012).
[33] B. Mansart, D. Boschetto, A. Savoia, F. Rullier-Albenque, F. Bouquet, E. Papalazarou, A. Forget, D. Colson, A. Rousse, and M. Marsi, Phys. Rev. B **82**, 024513 (2010).
[34] B. Mansart, D. Boschetto, A. Savoia, F. Rullier-Albenque, A. Forget, D. Colson, A. Rousse, and M. Marsi, Phys. Rev. B **80**, 172504 (2009).
[35] T. Mertelj, V. V. Kabanov, C. Gadermaier, N. D. Zhigadlo, S. Katrych, J. Karpinski, and D. Mihailovic, Phys. Rev. Lett. **102**, 117002 (2009).
[36] H. Takahashi, Y. Kamihara, H. Koguchi, T. Atou, H. Hosono, I. Katayama, J. Takeda, M. Kitajima, and K. G Nakamura, J. Phys. Soc. Jpn. **80**, 013707 (2011).
[37] L. Rettig, S. Mariager, A. Ferrer, S. Grübel, J. Johnson, J. Rittmann, T. Wolf, S. Johnson, G. Ingold, P. Beaud *et al.*, Phys. Rev. Lett. **114**, 067402 (2015).
[38] S. Gerber, K. W. Kim, Y. Zhang, D. Zhu, N. Plonka, M. Yi, G. L. Dakovski, D. Leuenberger, P. S. Kirchmann, R. G. Moore *et al.*, Nat. Commun. **6**, 7377 (2015).
[39] R. Merlin, Solid State Commun. **102**, 207 (1997).
[40] D. M. Riffe and A. J. Sabbah, Phys. Rev. B **76**, 085207 (2007).
[41] T. G. Pedersen, K. Pedersen, and T. B. Kriestensen, Phys. Rev. B **63**, 201101 (2001).
[42] M. Daghofer, A. Nicholson, A. Moreo, and E. Dagotto, Phys. Rev. B **81**, 014511 (2010).
[43] I. I. Mazin, D. J. Singh, M. D. Johannes, and M. H. Du, Phys. Rev. Lett. **101**, 057003 (2008).
[44] K. Kuroki, S. Onari, R. Arita, H. Usui, Y. Tanaka, H. Kontani, and H. Aoki, Phys. Rev. Lett. **101**, 087004 (2008).
[45] A. V. Chubukov, D. V. Efremov, and I. Eremin, Phys. Rev. B **78**, 134512 (2008).
[46] K. Seo, B. A. Bernevig, and J. Hu, Phys. Rev. Lett. **101**, 206404 (2008).
[47] C. Fang, Y.-L. Wu, R. Thomale, B. A. Bernevig, and J. Hu, Phys. Rev. X **1**, 011009 (2011).
[48] H. Kontani and S. Onari, Phys. Rev. Lett. **104**, 157001 (2010).
[49] R. Thomale, C. Platt, W. Hanke, J. Hu, and B. A. Bernevig, Phys. Rev. Lett. **107**, 117001 (2011).
[50] T. A. Maier, S. Graser, P. J. Hirschfeld, and D. J. Scalapino, Phys. Rev. B **83**, 100515(R) (2011).
[51] X. Lu, C. Fang, W.-F. Tsai, Y. Jiang, and J. Hu, Phys. Rev. B **85**, 054505 (2012).
[52] N. Hao and J. Hu, Phys. Rev. B **89**, 045144 (2014).
[53] J. Hu, Phys. Rev. X **3**, 031004 (2013).
[54] Z. Yin, K. Haule, and G. Kotliar, Nat. Phys. **10**, 845 (2014).